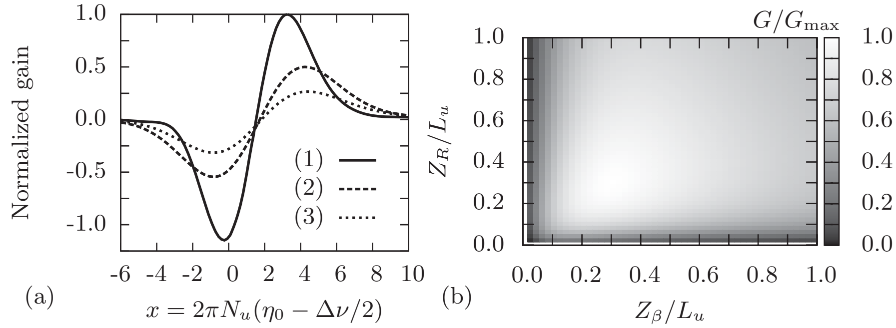

Figure 5.8 (a) Gain curves as a function of the scaled frequency detuning x for (1) $\varepsilon_x = \lambda_1/4\pi$, $\sigma_\eta = 1/6N_u$; (2) $\varepsilon_x = \lambda_1/4\pi$, $\sigma_\eta = 1/3N_u$; and (3) $\varepsilon_x = \lambda_1/2\pi$, $\sigma_\eta = 1/3N_u$. The radiation Rayleigh range Z_R and beam focusing Z_β have been chosen to maximize G, which has been normalized to the maximum gain of (1). (b) Normalized gain, maximized over $\Delta\nu$, plotted as a function of Z_β/L_u and Z_R/L_u for $\varepsilon_x = \lambda_1/4\pi$ and $\sigma_\eta = 1/2N_u$.

Table 5.1 Representative parameters of recent SASE FEL experiments and facilities whose ouput wavelength is less then 1 micron.

Parameters	VISA	LEUTL	FLASH	LCLS	SACLA	FERMI
γmc^2 [GeV]	0.071	0.22	1.1	13.64	6.135	1.2
σ_γ/γ [%]	0.17	0.2	0.03	0.01	0.01	0.015
I [kA]	0.25	0.2	2	3	3	0.8
$\varepsilon_{x,n}$ [μm]	3	5	2	0.4	0.85	0.8
$\bar{\beta}_x$ [m]	0.3	1.5	4.5	30	30	8
λ_u [cm]	1.8	3.3	2.7	2.7	1.5	3.5
K	1.2	3.1	1.2	3.5	1.36	$\sim$1
L_u [m]	4	20	27	100	100	20
min. λ_1 [nm]	830	530	6	0.15	0.1	4
Pulse length	1 ps	2 ps	30 fs	$\sim$70 fs	$\sim$100 fs	$<$100 fs

5.5 Solution in the High-Gain Regime

A high-quality beam in a sufficiently long undulator can produce FEL radiation that grows exponentially along the length of the undulator. In this high-gain regime the growing modes tend to dominate the FEL dynamics. We compile in Table 5.1 an incomplete list of high-gain, SASE-based experiments and facilities that have generated intense FEL output at wavelengths below 1 micron.[3]. Note the relevant electron beam parameters.

To analyze high-gain devices, it is convenient for our analysis to scale the field

[3] Several other FEL experimental facilities are listed in Table 8.1

variables according to

$$a_\nu = \frac{\chi_1}{2k_u\rho^2}E_\nu = \frac{eK[\mathrm{JJ}]}{4\gamma_r^2 mc^2 k_u\rho^2}E_\nu, \qquad f_\nu = \frac{2k_u\rho^2}{k_1}F_\nu. \tag{5.93}$$

The electromagnetic scaling is identical to that of Ch. 3, so that we anticipate saturation when

$$\frac{P_{\mathrm{rad}}}{\rho P_{\mathrm{beam}}} = \frac{\lambda_1}{cT}\left\langle \int d\nu d\boldsymbol{x}\; |a_\nu(\hat{z})|^2 \right\rangle \sim 1, \tag{5.94}$$

where $P_{\mathrm{beam}} = (I/e)\gamma_r mc^2$ is the electron beam power for a beam of peak current I. The distribution function scaling preserves $\int d\hat{p}\; f_\nu$ if we also introduce the dimensionless coordinates

$$\hat{z} = 2\rho k_u z \qquad \hat{\eta} = \frac{\eta}{\rho},$$
$$\hat{\boldsymbol{x}} = \boldsymbol{x}\sqrt{2k_1k_u\rho} \qquad \hat{\boldsymbol{p}} = \boldsymbol{p}\sqrt{\frac{k_1}{2k_u\rho}}. \tag{5.95}$$

Note that the scaled propagation distance and energy are identical to that introduced in the 1D analysis, while the transverse scaling is set so that the scaled rms radiation size and divergence are of order unity, with $\sigma_r\sigma_{r'} \sim 1/k_1$. In terms of these dimensionless variables, the governing FEL equations (5.62)-(5.63) are

$$\left(\frac{\partial}{\partial\hat{z}} + i\frac{\Delta\nu}{2\rho} + \frac{\hat{\boldsymbol{\nabla}}_\perp^2}{2i}\right) a_\nu(\hat{\boldsymbol{x}};\hat{z}) = -\int d\hat{\eta} d\hat{\boldsymbol{p}}\; f_\nu(\hat{\eta},\hat{\boldsymbol{x}},\hat{\boldsymbol{p}};\hat{z}) \tag{5.96}$$

$$\left(\frac{\partial}{\partial\hat{z}} + i\nu\dot{\theta} + \hat{\boldsymbol{p}}\cdot\frac{\partial}{\partial\hat{\boldsymbol{x}}} - \hat{k}_\beta^2\hat{\boldsymbol{x}}\frac{\partial}{\partial\hat{\boldsymbol{p}}}\right) f_\nu = -a_\nu\frac{\partial\bar{f}_0}{\partial\hat{\eta}}, \tag{5.97}$$

where the phase derivative

$$\dot{\theta} = \frac{d\theta}{d\hat{z}} = \hat{\eta} - \frac{\hat{p}^2 + \hat{k}_\beta^2\hat{\boldsymbol{x}}^2}{2} \tag{5.98}$$

describes the inhomogeneous effects of energy spread and emittance, and $\hat{k}_\beta = k_\beta/(2k_u\rho)$ is the scaled focusing strength.

5.5.1 Van Kampen's Normal Mode Expansion

In our previous analysis of the high-gain FEL, we found that there are typically three independent linear solutions in the 1D problem, one of which is the exponentially growing mode that dominates the long-distance dynamics. We would like to find a similar set of linear modes for the FEL in 3D, although in this case the mathematics is a bit more involved. First, there is the complication that in 3D there can be many (possibly infinitely many) growing modes. Second, the linear system (5.96)-(5.97) is not self-adjoint, so that the modes we find are not necessarily orthogonal. Van Kampen's normal mode expansion deals with these